A HEURISTIC MODEL FOR PLANNING OF SINGLE WIRE EARTH RETURN POWER DISTRIBUTION SYSTEMS

Geofrey Bakkabulindi[1*], Mohammad R. Hesamzadeh[2], Mikael Amelin[2], Izael P. Da Silva[1], Eriabu Lugujjo[1]
[1]Makererere University
P. O. Box 7062, Kampala, Uganda.
[2]Royal Institute of Technology
Teknikringen 33, Stockholm, Sweden.
[1*]Email: gbakkabulindi@tech.mak.ac.ug

ABSTRACT
The planning of distribution networks with earth return is highly dependent on the ground's electrical properties. This study incorporates a load flow algorithm for Single Wire Earth Return (SWER) networks into the planning of such systems. The earth's variable conductive properties are modelled into the load flow algorithm and the model considers load growth over different time periods. It includes optimal conductor selection for the SWER system and can also be used to forecast when an initially selected conductor will need to be upgraded. The planning procedure is based on indices derived through an iterative heuristic process that aims to minimise losses and investment costs subject to load flow constraints. A case study in Uganda was used to test the model's practical application.

KEY WORDS
Power distribution planning, Power flow analysis, Single Wire Earth Return, Rural electrification

1. Introduction

Since the pioneering work on Single Wire Earth Return (SWER) by Lloyd Mandeno in 1925 [1], the technology has proven to be very cost effective in electrifying scattered rural areas. Countries like New Zealand, Australia, Brazil and South Africa, among others, have several thousand kilometres of SWER lines installed with several lines having been in operation for well over 25 years [2]. However, many developing countries especially in sub-Saharan Africa have yet to mainstream SWER into their distribution networks despite prevailing low electrification rates. The major challenges facing these countries are lack of awareness, insufficient capacity for the required technical analysis and implementation as well as inadequate framework within which to design and plan these low-cost networks [3].

Considerable research has been done on SWER systems [1 - 3, 5, 9 -12] as well as power distribution system planning [4, 14, 15]. However, the planning of SWER distribution systems based on earth return load flow constraints has not been widely covered. The general objective of the distribution planning is to minimise the capital investment and operation costs of distribution substations and feeders to create a network that meets the projected load growth reliably and securely. This is achieved only if the constraints associated with equipment capacities, voltage limits, technical losses, and radial configuration are met [4]. SWER distribution systems use the earth as current return path. As such, the planning of these networks largely depends on an area's ground conductive properties which are, in turn, a function of soil type and humidity [5].

By using a heuristic approach, this paper presents a simple iterative procedure for planning SWER distribution systems. A dynamic planning model is used to consider the impact of load growth over several time periods on system performance. By using a load flow algorithm for earth return networks, optimal conductor selection is carried out for the initial case and the algorithm presents the possibility to determine when the initial conductor will need upgrade. The aim was to minimise the costs of distribution losses, initial installation costs for feeders and subsequent upgrades subject to load flow constraints. The model is applied to a case study in Uganda to test its performance. All mathematical model formulations were done using the General Algebraic Modelling System (GAMS).

2. System Model Formulation

2.1 SWER Distribution Line Model

The SWER distribution line model was based on Carson's line [6]. This model considers a single conductor parallel to the earth with unit length and carrying a current with return path through the ground. The earth return is considered to be a single conductor beneath the earth's surface with 1 m geometric mean radius (GMR), uniform resistivity and infinite length [5, 6]. The geometric mean distance (GMD) between the overhead conductor and the earth return path is a function of the soil resistivity, ρ [5, 7]. The total impedance, Z_{aa}, of the overhead line as a result of the earth presence was derived in [5] and is given by (1). The ground self impedance, z_{gg}, and the mutual impedance, z_{ag}, between the earth return and the phase conductor are given by (2) and (3) [5, 7].

$$Z_{aa} = \bar{z}_{aa} + \bar{z}_{gg} - 2\bar{z}_{ag} \quad (1)$$

$$\bar{z}_{gg} = \pi^2 \times 10^{-4} f - j0.0386 \cdot 8\pi \cdot 10^4 f + j4\pi \cdot 10^{-4} \cdot f \cdot ln(\frac{2}{5.6198 \cdot 10^{-3}}) \quad (2)$$

$$\bar{z}_{ag} = j2\pi \cdot 10^{-4} \cdot ln \frac{h_a}{\sqrt{\rho / f}} \quad (3)$$

Where f is the network frequency, h_a is the height of the overhead line in meters and the units of (1) to (3) are Ω/km. The self impedance of the overhead line was calculated using the Simplified Carson Method given by (4) [5, 8]. The details of the full development of the Carson line model are not included here for brevity but can be found in [5, 6, 8].

$$\bar{z}_{aa} = r_a + j4\pi \times 10^{-4} f \cdot ln\left(\frac{2h_a}{GMR_a}\right) \Omega/\text{km} \quad (4)$$

Where, r_a is the resistance of the phase conductor a (Ω/km) and GMR_a is the geometric mean radius of conductor a (m). The impedances of the sending and receiving earth connections were considered to be negligible compared to the conductor and ground values.

SWER lines are characterised by long span lengths since they supply scattered rural loads spread over large distances. As a result, line charging currents due to the Ferranti effect are quite pronounced in these systems compared to conventional distribution lines [9]. The voltage rise with distance results into voltage regulation problems at distant consumer load points [10]. The line shunt admittance, Y, normally neglected in conventional distribution lines was included in the line model to reflect the above phenomenon. The overhead line shunt capacitance, C, was computed using (5) [8]. Equation (5) was used to compute the capacitive reactance from which the shunt admittance was then derived.

$$C = \frac{2\pi\varepsilon_o}{ln\left(\frac{2h_a}{GMR_a}\right)} \quad (5)$$

2.2 Load Model

All loads were modelled as constant power loads. It was assumed that the loads were proportional to the sizes of the distribution transformers with a power factor of 0.8 lagging. As such, changes in power factor due to transformer inductances as well as losses due to the distribution transformers were considered as part of the load while ignoring voltage drops beyond the transformers to customer points [11].

3. Load Flow Algorithm

Although SWER lines can be connected directly to the rest of the three-phase distribution grid, an isolation transformer is often used to electrically isolate them from their energising feeders. This allows earth leakage protection to be used on the rest of the network and ensures that the energising feeders do not carry zero sequence currents [12]. In this study, an infinite bus was added at the isolating transformer output terminals to form the slack bus [11]. The isolation transformer itself was not included in the model. The load flow algorithm was based on the forward/backward sweep method whose steps are as explained below [13].

In the first step all nodal current injections due to loads, capacitor banks, if any, and shunt elements are calculated based on initial voltages. In subsequent iterations, updated voltages are used to calculate the nodal currents. For the single wire earth return case, the calculation of nodal currents is given by (6) [5].

$$\begin{bmatrix} I_{ia} \\ I_{ig} \end{bmatrix}^{(k)} = \begin{bmatrix} (S_{ia} / V_{ia}^{(k-1)})* \\ -I_{ia}^{(k)} \end{bmatrix} - \begin{bmatrix} Y_{ia} \\ 0 \end{bmatrix} \begin{bmatrix} V_{ia} \\ V_{ig} \end{bmatrix}^{(k-1)} \quad (6)$$

Where, I_{ia} and I_{ig} are the current injections at node i for the overhead line and earth return respectively, S_{ia} is the specified complex power load at node i, V_{ia} and V_{ig} are the complex voltages at node i for the overhead conductor and earth return respectively, Y_{ia} is the shunt admittance of the overhead line at node I, and k refers to the iteration index.

The second step is the backward sweep which calculates branch currents starting from the end nodes of the radial distribution network (RDN) backwards to the source node following Kirchoff's Current Law (KCL) [13]. The current, J, flowing through branch l is calculated according to (7) [5].

$$\begin{bmatrix} J_{la} \\ J_{lg} \end{bmatrix}^{(k)} = -\begin{bmatrix} I_{ja} \\ I_{jg} \end{bmatrix}^{k} + \sum_{m \in M} \begin{bmatrix} J_{ma} \\ J_{mg} \end{bmatrix}^{k} \quad (7)$$

Where, j is the end node of branch l and M is the set of all branches connected downstream from node j. A branch-to-node matrix was used to keep track of all the branches and nodes connected downstream from any branch.

In the third step, the forward sweep, bus voltages are updated using the current values obtained from the backward sweep starting at the root node towards the end nodes [13]. Nodal voltage calculations in the forward sweep were calculated using (8) [5].

$$\begin{bmatrix} V_{ja} \\ V_{jg} \end{bmatrix}^{(k)} = \begin{bmatrix} V_{ia} \\ V_{ig} \end{bmatrix}^{k} - \begin{bmatrix} Z_{aa} & Z_{ag} \\ Z_{ag} & Z_{gg} \end{bmatrix} \begin{bmatrix} J_{la} \\ J_{lg} \end{bmatrix}^{k} \quad (8)$$

Where, i and j are the incoming and outgoing nodes of branch l respectively. The impedances are calculated as in (1) to (4).

The above method was formulated as an optimisation algorithm in GAMS to obtain a solution to the network load flow following convergence. The objective of the optimisation was to minimise the difference between the specified and calculated load power injections at each bus [5] subject to the constraints given in (6) to (8). The objective function formulations to be minimised for the earth return load flow solution are given in (9) and (10).

$$\Delta S_{ia}^{k} = V_{ia}^{k}(I_{ia}^{k})^{*} - Y_{ia}^{*}\left|V_{ia}^{k}\right|^{2} - S_{ia} \quad (9)$$

$$\Delta S_{ig}^{k} = V_{ig}^{k}(I_{ig}^{k})^{*} \quad (10)$$

All parameters and variables in (6) to (10) are complex.

4. Methodology

A forward planning approach was used in the planning model. Using an iterative process shown in figure 1, the load flow algorithm developed above was used to test different system scenarios. Performance indices were formulated to test the suitability of each scenario starting from a base case and multiple simulations of the load flow algorithm were used to test each case. The performance of different feeders was measured against load growth for different time periods, t, up to the horizon year of the planning period, t_{max}. This was in turn used to determine the need for upgrade on existing feeders and the time period during which this would be required, if at all. The annual load growth was calculated using (11) [14].

$$S_t = S_o \times (1+g)^t \quad (11)$$

Where S_t is the load after time t in years, S_o is the initial load in the base year, g is the percentage annual load growth rate and t is the number of years.

The planning algorithm was intended to identify the branches exhibiting weak points in the network given load growth. The performance indices were based on voltage profile, feeder losses, conductor utilisation and cost. The different indices were combined using an overall index which reflected the proportional contribution of each index to the general system performance. The above approach is summarised in figure 1.

The proposed procedure was based on the assumption that only the peak load was considered for the successive time periods. Furthermore, it was assumed that the feeder route and different conductor options were known in advance and their costs of installation estimated.

4.1 Voltage index

An index for the voltage profile was developed to monitor the node voltage deviations for different conductor options given increasing load. This index, given by (12), was formulated as the difference between the actual bus voltage magnitude and the nominal voltage, V_o (1 p.u), in a given time period using conductor c [15].

$$I_{volt,c} = \frac{\sum_{i=1}^{n}\sum_{t=1}^{t_{max}}\left|V_{i,t,c} - V_o\right|}{n \cdot t_{max}} \times 100\% \quad (12)$$

Where $I_{volt,c}$ is the voltage index for conductor c, $V_{i,t,c}$ is the actual voltage at bus i using conductor c, t_{max} is the total number of years in the planning period and n is the total number of buses on the network.

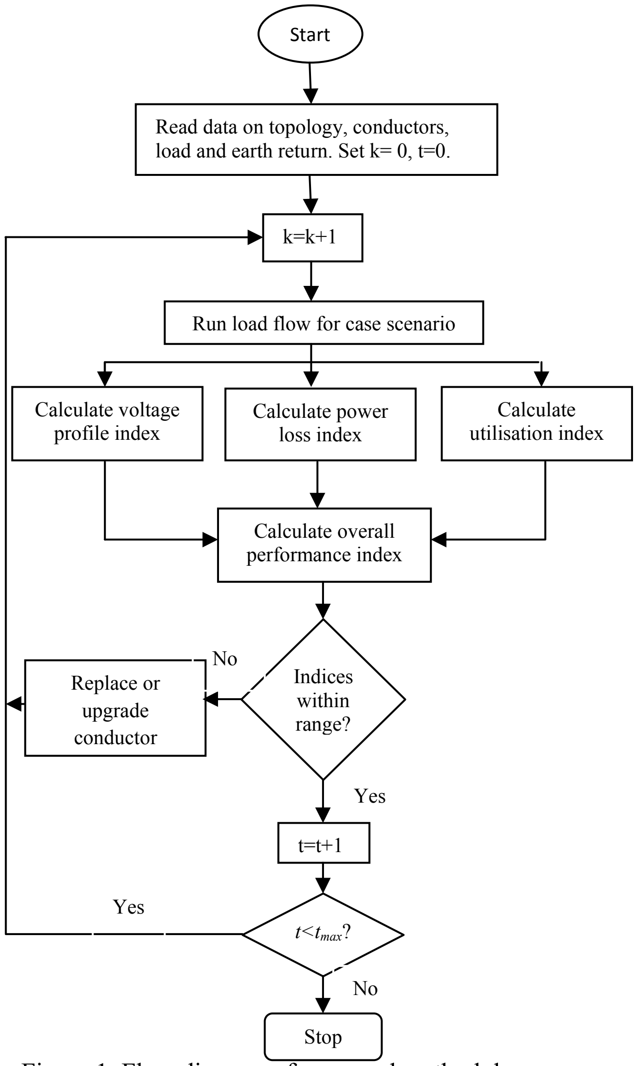

Figure 1. Flow diagram of proposed methodology

The allowable voltage limits for SWER distribution transformers are slightly different from those of ordinary distribution transformers and should be within the range 0.907 to 1.027 p.u [11]. The voltage index in (12) was only used for bus voltages within that range. It follows that the smaller the overall voltage deviation from the nominal 1 p.u, the better the system performance.

4.2 Conductor Utilisation Index

This index was formulated as a measure of conductor capacity usage compared to rated current carrying limits. It was intended to determine overloaded lines during the planning process. In addition, this index would help determine if a conductor was using too little of its capacity during the planning period leading to unnecessarily high investment costs. The index, given by (13), was developed using line current flows obtained from the load flow simulations.

The ratios of the branch current flows from the load flow to the rated conductor current carrying limits were used to identify the current loadings on specific segments. The index only considered branch segments whose current flows throughout the planning period were within their thermal limits. It follows, therefore, that the higher the utilisation index for a given conductor, the better its performance in supplying the peak load.

$$I_{u,c} = \frac{\sum_{l=1}^{nl}\sum_{t=1}^{t_{max}} (J_{l,t,c} / J_{max,c})}{nl \cdot t_{max}} \times 100\% \qquad (13)$$

Where $I_{u,c}$ is the utilisation index using conductor c, $J_{l,t,c}$ is the average current flowing through branch l during year t using conductor c, $J_{max,c}$ is the thermal limit of conductor c, nl is the total number of branches in the network and t_{max} is the total number of years in the planning period.

4.3 Power Loss Index

The power loss index was developed to check the technical losses associated with different conductor options for the earth return system. The index, given by (14), was developed based on the system losses as a ratio of total active power demand.

$$I_{loss,c} = \frac{\sum_{l=1}^{nl}\sum_{t=1}^{t_{max}} (J_{l,t,c}^{2} \cdot R_{l,c})}{\sum_{i=1}^{n}\sum_{t=1}^{t_{max}} P_{i,t}} \times 100\% \qquad (14)$$

Where $R_{l,c}$ is the resultant resistance in branch l due to the overhead conductor c and earth return path as derived in (1). $P_{i,t}$ is the active power demand at node i during time period t. It is desired to have minimum network losses and therefore, the lower the loss index the better the performance of a given conductor.

4.4 Overall Index

An overall index was formulated to combine the different indices formulated in (12) to (14). The voltage index tracks the voltage deviations for each option and therefore, for good system performance, it should be as small as possible. This implies an inverse relationship between this index and the overall performance index.

The conductor utilisation index measures conductor usage compared to thermal limits during the planning period. Better conductor utilisation within thermal limits implies better system performance and optimised conductor cost. Therefore, the utilisation index has direct proportionality with the overall performance index.

Lower power losses in the system lead to better system performance. Therefore, the power loss index has an inverse relationship with the overall performance index. The above relationships are formulated in (15) with the proportionality constant formulated as the square of the present value of investment cost.

$$I_{o,c} = \frac{I_{u,c}}{I_{volt,c} \cdot I_{loss,c} \cdot C_c^2} \times 100\% \qquad (15)$$

Where $I_{o,c}$ is the overall index for conductor c and C_c is the present value of investment cost of conductor c.

5. Application

5.1 Case Study

The case study was done in Ntenjeru county, Mukono district in central Uganda. The area was selected because it is largely rural and vast areas of it lay un-electrified at the time of this study. However, it had proximity to the national grid and thus the possibility to be electrified cost-effectively using SWER. All data pertaining to the proposed distribution network was collected locally during field surveys. Such data included potential load demand in villages, soil resistivity, network topology, etc.

5.2 Proposed Test Network

The proposed network topology was based on the potential electrical load estimates of the main load centers determined during previous field surveys. The loads consisted of villages, farms, schools, trading centers and health centers. Ugandan rural loads are characterized by low energy consumption with the main energy source being biomass [16]. However, electrification often acts as a stimulant for economic activities subsequently leading to rapid load growth.

In the proposed RDN, a 33 kV grid was considered located in Ntenjeru town and at that point an infinite bus was connected. The majority of the load centers were located along the existing roads. It was considered that the SWER line would run along the roads to ease customer connections and line maintenance. Owing to this and the relatively large distances between load centers, a network routing algorithm was not formulated.

The proposed network shown in figure 2 had 18 load points modeled as described in section 2.2. Soil resistivity measurements were done using the Wenner Four Pin Method [17] for different locations and times. The average soil resistivity, ρ, was found to be approximately 400 ohm.m. Additional network data are given in tables 1 and 2.

The node indexing scheme used for the network in figure 2 was that proposed in [14]. The nodes on the primary feeder were numbered first followed by those on the laterals whereas the branches were numbered according to their outgoing nodes as in table 2. This numbering scheme facilitated the forward/backward sweep method in the load flow calculation for the RDN.

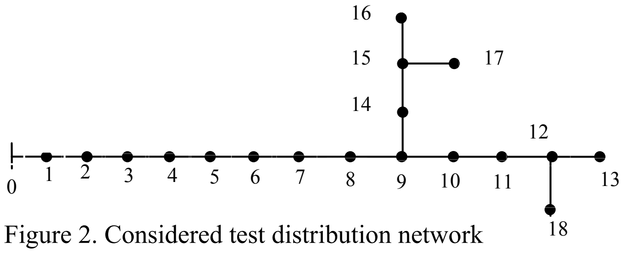

Figure 2. Considered test distribution network

Table 1
Bus indices and loads for the considered SWER RDN

Bus	Demand (kVA)	Bus	Demand (kVA)
0	0	10	16
1	32	11	16
2	16	12	16
3	32	13	32
4	32	14	32
5	16	15	32
6	16	16	32
7	16	17	32
8	32	18	32
9	32	Total	240

Table 2
Branch information for considered SWER RDN

Bus *i*	Bus *j*	Branch index	Branch length (km)
0	1	1	1.0
1	2	2	1.4
2	3	3	1.9
3	4	4	1.3
4	5	5	2.5
5	6	6	0.5
6	7	7	0.7
7	8	8	2.0
8	9	9	2.5
9	10	10	1.6
10	11	11	2.4
11	12	12	1.2
12	13	13	0.9
9	14	14	3.0
14	15	15	1.2
15	16	16	2.1
15	17	17	4.4
12	18	18	1.0
Total distance			31.5

5.3 Load Flow Calculation

The load growth for rural areas in Uganda was estimated at 5% following electrification. The planning period for the test network excluding the base year was chosen to be 5 years for illustration. SWER system impedances were calculated as described in 2.1 for the different conductors using the measured average soil resistivity. Table 3 shows some of the electrical properties of the different conductors used in the study. All resistances were obtained for 75°C. The conductors were chosen because of their low cost, light weight and high tensile strength which allows longer span lengths.

The general system data are: f=50 Hz, ρ = 400 Ωm, impedance of earth return 'conductor', Z_{gg} = (0.0493 + j0.3643) Ω/km, the mutual impedance between single wire and earth was considered negligible. The base and reference voltages were considered as 19.1 kV which is the phase to ground voltage of the 33 kV 3-phase supply. The base power was chosen as 100 kVA. The conductor costs were considered to be roughly proportional to their thermal capacities (table 3). The load demand factor was assumed to be 1 and power factor 0.8.

.

Table 3
Electrical properties of considered conductors

Conductor code		R (Ω/km)	X (Ω/km)	Current rating (A)
1	Bantam	5.26	1.02	69
2	3/2.75 SC/GZ	12.55	1.00	38
3	Mole	3.30	1.03	98
4	Magpie	3.31	0.99	92
5	Shrike	2.08	0.96	122
6	Squirrel	1.67	0.99	148
7	Snipe	1.31	0.93	162
8	Loon	1.04	0.92	186

5.4 Results and Discussion

5.4.1 Conductor Selection

The proposed iterative algorithm was applied to the conductors in table 1 to determine the optimal conductor for the network in the base case. The objective was to select the conductor whose electrical properties would be sufficient to meet the peak load in an economical and secure way throughout the planning period. Table 4 shows the obtained performance results obtained using the indices formulated in section 4.

The results in table 4 were calculated over the chosen 10 year period with 5% load growth. The SC/GZ conductor had the poorest overall performance index. Despite being the cheapest option, its phase voltage profile at distant buses dropped well below 0.8 p.u as shown in figure 3 and so it also had the highest losses. This can be attributed to its high R/X ratio. Any installation of the SC/GZ conductor in the case study area would have to be upgraded in the fifth year when the branch current flow would exceed its thermal limit as shown in figure 5.

Table 4
Performance indices for different network conductors in 10 year planning period

Conductor Code	$I_{volt,c}$ (%)	$I_{u,c}$ (%)	$I_{loss,c}$ (%)	$I_{o,c}$ (%)
Bantam	7.74	23.35	11.96	1.84
3/2.75 SC/GZ	22.87	34.12	52.35	0.71
Mole	5.11	15.81	6.98	1.58
Magpie	5.09	16.82	6.98	**1.97**
Shrike	3.53	12.40	4.23	1.91
Squirrel	3.06	10.16	3.37	1.54
Snipe	2.58	9.21	2.63	1.80
Loon	2.25	7.98	2.09	1.70

The 'Magpie' conductor, however, had the highest overall performance attributed to its lower R/X ratio, low losses, sufficient thermal capacity allowing small voltage deviations and moderate cost. This made it the best choice for the initial conductor selection. Figure 3 shows the overhead phase to ground voltage profiles of the eight conductors in the 10th or horizon year. The annual losses of the conductors were calculated using (16) and figure 4 shows their trend over the planning period at 5% load growth. Figure 5 shows conductor utilization as a ratio of thermal capacity for each conductor in branch 1 which has the highest current flow magnitude.

$$Loss_{t,c} = \sum_{l=1}^{nl} J_{l,t,c}^{2} \cdot R_{l,c} \qquad (16)$$

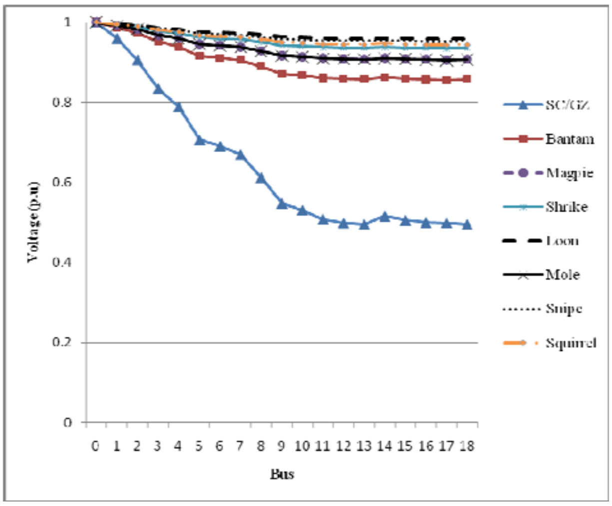

Figure 3. Overhead phase to ground voltage profiles in the 10th year for different conductors

5.4.2 Sensitivity Analysis

The conductors were subjected to load growth scenarios categorized under low, base and high to test their performance under different conditions. The low demand

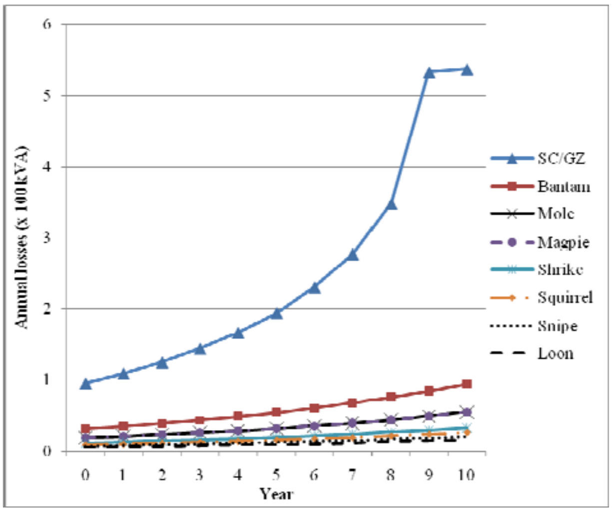

Figure 4. Annual losses for different conductors during 10 year planning period at 5% load growth

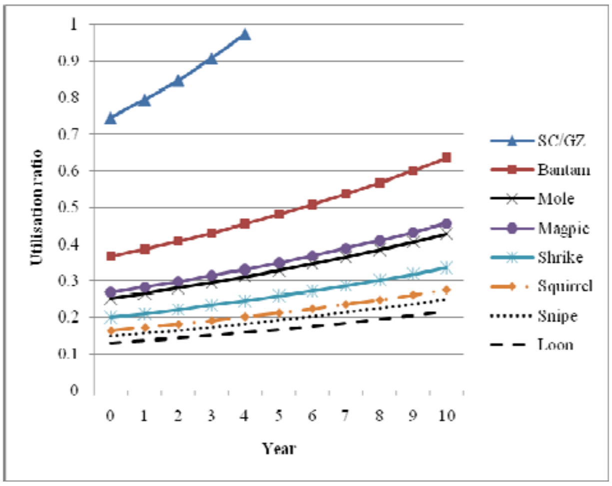

Figure 5. Conductor utilization during 10 year planning period at 5% load growth

scenario was 3%, the base scenario 5% and the high demand scenario 10%. The base rural demand scenario was chosen to be slightly lower than Uganda's average annual GDP growth rate of 7% [16]. The high demand scenario was tied to the possibility of rapid economic growth. Furthermore, a longer planning period of 15 years was considered for the sensitivity analysis to investigate conductor performance beyond the previously considered period. Table 5 shows the overall performance indices for all conductors operating under the different scenarios above.

It can be observed from table 5 that the Magpie conductor gave the best overall performance in both low and base demand scenarios for the 15 year period. However, with 10% load growth in the same period, the Shrike conductor outperforms Magpie due to its larger size. GAMS simulations indicated that for 10% growth, Magpie would get overloaded in the 13th year thus requiring an upgrade to Shrike or a larger conductor.

Table 5
Conductor performance for different load growth scenarios in 15 year planning period

Conductor Code	$I_{o,c}$, 3%	$I_{o,c}$, 5%	$I_{o,c}$, 10%
Bantam	1.92	1.47	0.27
3/2.75 SC/GZ	0.90	0.46	0.17
Mole	1.64	1.29	0.49
Magpie	2.05	1.62	0.59
Shrike	1.98	1.58	**0.80**
Squirrel	1.59	1.28	0.66
Snipe	1.86	1.50	0.78
Loon	1.76	1.42	0.75

The total primary feeder length of the proposed network (19.9 km) was relatively short and therefore the impact of the Ferranti effect was not fully reflected in the model results. Figure 6 shows the variation of ground voltages with time at 5% growth for Magpie over 10 years. Since the ground forms the current return path, ground voltages increase along the length of the network from the source bus as depicted in figure 6. The voltages likewise increase with load growth due to increased current flows. The opposite would be true for longer SWER feeders where the higher shunt capacitances due to the Ferranti effect would increase the distributed charging currents. This would cause the network to draw less current from the source with load growth [17].

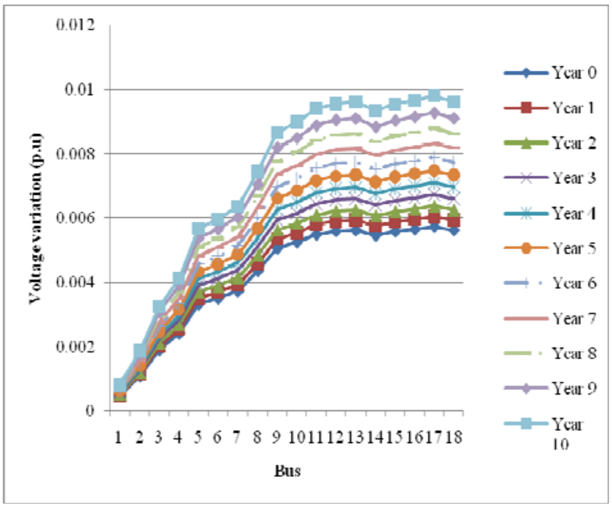

Figure 6. Ground voltage variation with time at 5% load growth over 10 years for Magpie conductor.

6. Conclusion

A planning algorithm for SWER systems was formulated in this study based on a heuristic approach. The SWER system parameters of phase and ground conductors were modelled and a corresponding load flow algorithm formulated. The load flow simulations were used in an iterative procedure to determine conductor performances with load growth over different time periods. The procedure was used to optimise conductor selections for initial installation as well as upgrade of existing networks. This was accomplished through the formulation of appropriate performance indices. The proposed algorithm was applied to an un-electrified case study in Uganda and a sensitivity analysis revealed favourable results for the chosen option. The sensitivity analysis further gave a forecast of when upgrade would be needed for the chosen conductor in different demand growth scenarios and a possible upgrade conductor option.

Acknowledgments

The authors would like to thank the Swedish International Development Agency (Sida) for the financial support to undertake this research. Jochen Roeber of GS Fainsinger & Associates is gratefully acknowledged for providing useful practical information on SWER.

References

[1] L. Mandeno, “Rural Power Supply Especially in Back Country Areas”, Proceedings of the New Zealand Institute of Engineers, Vol 3, 1947, Ferguson and Osborn Printers, Wellington, pp 234-271.
[2] P. J. Wolfs, N. Hosseinzadeh, S. T. Senini, “Capacity Enhancement for Aging Single Wire Earth Return Distribution Systems”, IEEE Power Engineering Society Annual General Meeting, Tampa Florida, 24-28, June 2007.
[3] Energy Sector Management Assistance Program (ESMAP), “Sub-Saharan Africa: Introducing Low-cost Methods in Electricity Distribution Networks”, Technical paper 104/06, October 2006.
[4] M. C. Da Silva, P. M. Franca and P. D. B. Da Silveira, “Long-range Planning of Power Distribution Systems: Secondary Networks”, Elsevier Journal of Computers and Electrical Engineering, Vol 22, No. 3, pp. 179 – 191, 1996.
[5] R. M. Ciric, L. F. Ochoa, A. Padilha, “Power Flow in Distribution Networks with Earth Return”, Elsevier Journal of Electrical Power and Energy Systems, 26, 2004, 373 – 380.
[6] J. R. Carson, “Wave Propagation in Overhead Wires with Earth Return”, Bell Syst. Tech. J 1926.
[7] P. M. Anderson, “Analysis of faulted power systems”, New York: IEEE Press Power Systems Engineering Series, 1995, pp. 71 – 83.
[8] R. Horton, W. G. Sunderman, R. F. Arritt and R. C. Dugan, “Effects of Line Modeling Methods on Neutral-to-Earth Voltage Analysis of Multi-Grounded Distribution Feeders”, Proceedings of the Power Systems Conference and Exposition (PSCE), 2011 IEEE/PES, pp. 1 – 6.
[9] T. R. Brooking and N. J. V. Rensburg, “The Improved Utilisation of Existing Rural Networks with the use of Intermediate Voltage and Single Wire Earth Return Systems”, 1992, IEEE, pp. 228-234.
[10] P. J. Wolfs, “Capacity Improvements for Rural Single Wire Earth Return Systems”, Proceedings of the 7th International Power Engineering Conference, 2005.
[11] N. Hosseinzadeh and J. Rattray, “Economics of Upgrading SWER distribution Systems”, Proceedings of the Australian Universities Power Engineering Conference, 2008.

[12] N. Hosseinzadeh and S. Mastakov, “Load Modeling for Medium Voltage SWER Distribution Networks”, Australian Universities Power Engineering Conference Proceedings, 2008.
[13] Abdel-Akher, et al, “Development of Unbalanced Three-Phase Distribution Power Flow Analysis Using Sequence and Phase Components”, Proceedings of the 12th International Middle-East IEEE Power System Conference, 2008.
[14] R. Ranjan, B. Venkatesh and D. Das, “A new algorithm for power distribution planning”, Elsevier Journal of Electric Power Systems Research, 62, 2002, 55 – 65.
[15] K. Qian, C. Zhou, M. Allan and Y. Yuan, “Effect of load models on assessment of energy losses in distributed generation planning”, Elsevier Journal of Electrical Power and Energy Systems, 33, 2011, 1243 – 1250.
[16] Uganda Bureau of Statistics, “Statistical Abstract”, 2009.
[17] T. G. Hicks, H. Mahrous, A. H. Seidman, “Handbook of Electric Power Calculations”, McGraw-Hill Book Company, New York, 1983.